ORDER IN SUPPORTED PHOSPHOLIPID MONOLAYERS DETECTED BY THE DICHROISM OF FLUORESCENCE EXCITED WITH POLARIZED EVANESCENT ILLUMINATION

NANCY L. THOMPSON AND HARDEN M. MCCONNELL
Department of Chemistry, Stanford University, Stanford, California 94305

THOMAS P. BURGHARDT
Cardiovascular Research Institute, University of California at San Francisco, San Francisco, California 94143

ABSTRACT A technique is described and demonstrated for measuring the orientation distribution of fluorescent molecules in a two-dimensional system. A laser beam is totally internally reflected at the interface between a glass slide and an aqueous solution, which creates a thin layer of evanescent illumination that excites fluorescent molecules near the interface. Molecules with absorption dipoles at different tilts from the normal to the interface are preferentially excited when the laser polarization is rotated. Approximately one-half of the emitted fluorescence is collected with an inverted microscope using a high-aperture objective. The fluorescence vs. polarization curve yields the value of an order parameter that is related to the orientation distribution of absorption dipoles. This technique is applied to phospholipid monolayers made at an air/water interface and transferred to hydrophobic glass microscope slides. Dipalmitoylphosphatidylcholine monolayers were doped with 2 mol % phosphatidylethanolamine labeled with the fluorescent moiety nitrobenzoxadiazole, either on an acyl chain or on the head group. The measured value of the order parameter for the head-labeled probe decreases as a function of the surface pressure at which the monolayer is transferred to the slide, as the surface pressure increases from 10 to 40 dyne/cm. The measured value of the order parameter for the chain-labeled probe is high for all coating pressures. These results can be interpreted in terms of probe partitioning into coexistent fluid and solid domains. Dimyristoylphosphatidylcholine monolayers were doped with 2 mol % chain-labeled phosphatidylethanolamine, either free or covalently conjugated to a small peptide. In these monolayers, the measured value of the order parameter is high at all pressures. The technique presented here may also prove useful for measuring the orientation distribution of proteins bound to or embedded in a planar model membrane.

INTRODUCTION

One method of studying the process of cell-cell interaction in the immune system is to replace one of the interacting cells with a model phospholipid membrane. The model membrane may be presented to a cell in the form of a phospholipid vesicle (e.g., Balakrishnan et al., 1982; Cartwright et al., 1982) or as a planar phospholipid monolayer supported by a chemically modified glass slide (von Tscharner and McConnell, 1981*a*, *b*). Interactions between supported phospholipid monolayers and macrophages (Hafeman et al., 1981, 1984), neutrophils (Hafeman et al., 1982, 1984), basophils (Weis et al., 1982) and T cells (Nakanishi et al., 1983; Brian and McConnell, 1984; Watts et al., 1984) have been studied. These immunologically relevant experiments have raised interest in understanding more thoroughly the physical state of the supported monolayers (Seul et al., 1983) and of proteins or peptides (Thompson et al., 1984) that the monolayers incorporate. Molecular monolayers are also of interest in fields other than immunology, such as membrane biophysics, protein crystallography (Uzgiris and Kornberg, 1983), medical technology, optics (Drexhage, 1974; Kuhn et al., 1972), and surface physics (Barlow, 1980; Sinha, 1980).

In this paper, a technique is described for measuring the orientation distribution of the absorption dipoles of fluorescent-labeled phospholipids in a supported monolayer. A laser beam is totally internally reflected at the interface between the slide and the solution, which creates a thin layer of evanescent illumination that excites fluorescent molecules in or near the monolayer. The evanescent light propagates along the interface, and rotating the polarization of the laser rotates the evanescent electric field through directions parallel and perpendicular to the inter-

face. If one-half of the emitted fluorescence is collected, using an inverted microscope with a high-aperture objective, the fluorescence as a function of the direction of the polarization of the incident beam yields the value of an order parameter that depends only on the orientation distribution of absorption dipoles.

As discussed in the accompanying paper (Burghardt and Thompson, 1984*b*), less than one-half of the emitted fluorescence is collected. First, the angular distribution of emitted fluorescence is changed by the nearby presence of the glass slide. Second, even with the highest-aperture oil immersion microscope objectives, a solid angle of 2π is not observed because light is reflected at the oil-coverslip/water interface. These effects are accounted for in data analysis.

The orientation distribution of fluorescent probes in phosphatidylcholine monolayers has been investigated. Studies were done on dipalmitoylphosphatidylcholine monolayers containing a small amount of phosphatidylethanolamine labeled with the fluorescent moiety nitrobenzoxadiazole (NBD-PE) either on one acyl chain or at the head group, examined as a function of the surface pressure at the air/water interface before transfer to the slide. Studies were also done on dimyristoylphosphatidylcholine monolayers containing acyl chain-labeled NBD-PE, either free or conjugated to a small peptide (Thompson et al., 1984), examined as a function of the surface pressure at transfer.

Applications of total internal reflection fluorescence in the study of biologically relevant surface phenomena have recently been reviewed (Axelrod et al., 1984). Also, absorption dichroism as detected by fluorescence, using a focused laser beam, has been used to determine the orientation distribution of myosin cross-bridges in skeletal muscle fibers (Borejdo et al., 1982; Burghardt et al., 1983, 1984; Burghardt, 1984). The absorption of evanescent light in the infrared has been used to study oriented molecular films at an interface (e.g., Fluornoy and Schaffers, 1966; Harrick, 1967).

THEORY

In the experiments, a collection of fluorophores are located near a dielectric interface. A laser beam is totally internally reflected at the interface, which creates a thin layer of evanescent illumination that excites the molecules. Evanescent light absorption and subsequent emission and collection of fluorescence depends on the polarization of the incident beam and on the distribution of absorption dipole orientations. Below, we discuss (*a*) the absorption by, fluorescence emission of, and fluorescence collection from a single fluorophore, (*b*) a model-independent method of interpreting the fluorescence measured from a collection of fluorophores, and (*c*) a method of interpreting the measured data in terms of a particular model for the form of the distribution of absorption dipole orientations.

Absorption by, Emission of, and Collection from a Single Oriented Molecule

The coordinate system and parameters defined in Fig. 1 describe the evanescent electric field produced by a single, totally internally reflected plane wave. The xy plane is the interface of materials with refractive indices n_1 ($z > 0$) and n_2($z < 0$) and the relative index $n = n_1/n_2 < 1$. A plane wave has incidence plane xz, incidence angle α (greater than the critical angle $\alpha_c = \sin^{-1}n$), vacuum wavelength λ_0, and angular frequency ω, and is polarized at an angle ψ from the xz plane. The evanescent electric field incident on molecules at $z = 0$ on the interface is (Harrick, 1967; Born and Wolf, 1980):

$$\mathbf{E}_{x,y,z} = Re(\{[\mathcal{E}_x \cos\psi \exp[-i(\delta_\parallel + \pi/2)], \mathcal{E}_y \sin\psi \exp(-i\delta_\perp), \mathcal{E}_z \cos\psi \exp(-i\delta_\parallel)]\} \exp[i(kx - \omega t)]) \quad (1)$$

where

$$\mathcal{E}_x = 2\cos\alpha(\sin^2\alpha - n^2)^{1/2}/[n^4\cos^2\alpha + \sin^2\alpha - n^2]^{1/2};$$

$$\mathcal{E}_y = 2\cos\alpha/(1 - n^2)^{1/2};$$

$$\mathcal{E}_{z1,z2} = (1, n^2)\, 2\cos\alpha \sin\alpha/[n^4\cos^2\alpha + \sin^2\alpha - n^2]^{1/2};$$

$$\delta_{\parallel,\perp} = \tan^{-1}\{(\sin^2\alpha - n^2)^{1/2}/[(n^2, 1)\cos\alpha]\}; \quad (2)$$

$$k = 2\pi n_2 \sin\alpha/\lambda_0. \quad (3)$$

The refractive index of the monolayer is nearly equal to that of the glass (Drexhage, 1974; Fettiplace et al., 1975), so that total internal reflection actually occurs at the monolayer/solution interface. In Eq. 2, $\mathcal{E}_{z1}$ and $\mathcal{E}_{z2}$ are the amplitudes of the component of the electric field that are normal to the interface, in the n_1 (water) and n_2 (monolayer) regions, respectively. For a fluorescent probe on the

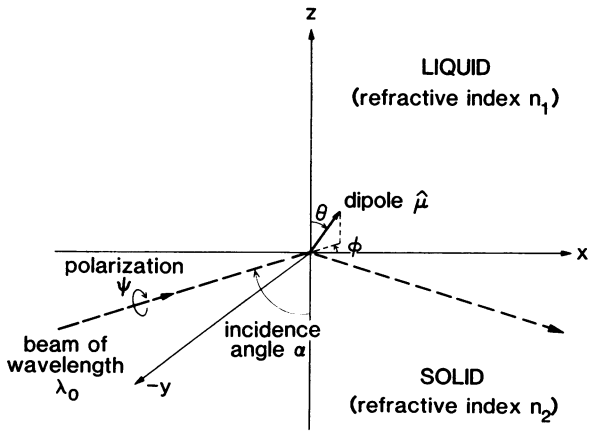

FIGURE 1 Excitation of fluorescent molecules with evanescent illumination. A plane wave of vacuum wavelength λ_0 is incident on the interface of a solid (refractive index n_2) and liquid (refractive index $n_1 < n_2$) at an angle α greater than the critical angle for total internal reflection. The interface is defined as the xy plane and the plane wave is incident in the xz plane. The plane wave is linearly polarized at an angle ψ from its incidence plane. A dipole $\hat{\mu}$ with polar and azimuthal angles θ and ϕ is excited by the evanescent illumination.

head group of a phospholipid, the normal component of the field is $\mathcal{E}_{z1}$, and for a fluorescent probe on the acyl chain, the normal component of the field is $\mathcal{E}_{z2}$. The tangential electric field amplitude, $\sqrt{\mathcal{E}_x^2 + \mathcal{E}_y^2}$, is continuous across the interface.

In the lower refractive index medium, the electric field is given by Eq. 1 with an overall multiplicative factor of $\exp(-z/2d)$. The depth of penetration d into the lower refractive index medium is:

$$d = \lambda_0/[4\pi n_2(\sin^2\alpha - n^2)^{1/2}]. \quad (4)$$

Examination of Eq. 1 indicates that an incident plane wave linearly polarized perpendicular ($\psi = 90°$) or parallel ($\psi = 0°$) to the incidence plane gives rise to an evanescent electric field that is also polarized perpendicular or parallel, respectively, to the incidence plane. However, although the perpendicular evanescent field is strictly linearly polarized (in the y direction), the parallel evanescent field has a polarization with components along both z and x. By calculating $\mathbf{E}$ in Eqs. 1–3 for $\psi = 0°$, one sees that the polarization rotates through the xz plane as a function of coordinate x and time t. The polarization is on the average more along z than along x.

In the experiments, a laser beam of Gaussian spatial intensity profile is focused by a lens on the interface at which it totally internally reflects. The polarization and penetration depth of the evanescent illumination are nearly equal to that created by a totally internally reflected plane wave (see Materials and Methods).

In these experiments, all dipoles are at $z = 0$. The absorption by a single dipole $\hat{\mu}$ oriented with polar angle θ and azimuthal angle ϕ (defined in Fig. 1) for an incident beam of polarization ψ is given by

$$\mathcal{A}(\theta, \phi, \psi) = \langle(\hat{\mu} \cdot \mathbf{E})^2\rangle, \quad (5)$$

where $\langle\ \rangle$ denotes a time average, and

$$\hat{\mu} = \sin\theta\cos\phi\,\hat{x} + \sin\theta\sin\phi\,\hat{y} + \cos\theta\,\hat{z}. \quad (6)$$

Using Eqs. 1 and 6 in Eq. 5 implies that

$$\mathcal{A}(\theta, \phi, \psi) = a + b\cos^2\psi + c\sin\psi\cos\psi, \quad (7)$$

where

$$\begin{aligned} a &= I_y \sin^2\theta \sin^2\phi \\ b &= (I_x\cos^2\phi - I_y\sin^2\phi)\sin^2\theta + I_z\cos^2\theta \\ c &= 2(I_{xy}\sin^2\theta\cos\phi + I_{yz}\cos\theta\sin\theta)\sin\phi \end{aligned} \quad (8)$$

and

$$\begin{aligned} I_{x,y,z} &= \mathcal{E}_{x,y,z}^2 \\ I_{xy} &= \mathcal{E}_x\,\mathcal{E}_y\sin(\delta_\perp - \delta_\parallel) \\ I_{yz} &= \mathcal{E}_y\,\mathcal{E}_z\cos(\delta_\perp - \delta_\parallel). \end{aligned} \quad (9)$$

Only a fraction of the fluorescence intensity emitted from a molecule is collected. If the objective collects a 2π solid angle, and if the fluorophores are in a dielectrically homogeneous medium, then one-half of the emitted fluorescence is collected, regardless of the orientation of the absorption and emission dipoles. However, as described fully in the accompanying paper (Burghardt and Thompson, 1984*b*), the fraction f depends on the orientation of the fluorophore because: (*a*) the glass-monolayer/water interface perturbs the angular intensity distribution of emitted fluorescence; and (*b*) the interface between the sample immersion (water) and the objective immersion (oil plus coverslip) does not transmit plane waves of different propagation and polarization directions with equal efficiencies.

For our application, and assuming that the absorption dipole is in the same direction as the emission dipole, the collection efficiency is given by (see accompanying paper):

$$f(\theta) \propto [1 - \gamma\cos^2\theta], \quad (10)$$

where θ is the polar angle of the absorption dipole, as shown in Fig. 1. Factor γ ranges from 1 to $-\infty$. If γ is positive (negative), then more (less) fluorescence is collected from a dipole oriented parallel to the interface than from one oriented perpendicular. In the accompanying paper, for the conditions of our experiments, it is shown that $\gamma = 0.10$ for a fluorophore at the interface in the water, and that $\gamma = 0.44$ for a fluorophore at the interface in the monolayer.

Model-Independent Absorption Dichroism Detected by Fluorescence

The evanescent illumination is incident on a collection of fluorophores at different orientations. In the steady state, the instantaneous distribution of absorption dipoles can be described by a time-independent function $N(\theta, \phi)$, normalized so that its integral over all angles is 1:

$$\int_0^{2\pi}\int_0^{\pi} N(\theta, \phi)\sin\theta d\theta d\phi = 1. \quad (11)$$

The total measured fluorescence $F(\psi)$ is

$$F(\psi) = \int_0^{2\pi}\int_0^{\pi} N(\theta, \phi)\mathcal{A}(\theta, \phi, \psi)f(\theta)\sin\theta d\theta d\phi. \quad (12)$$

Function $N(\theta, \phi)$ is expanded in a set of orthogonal functions, the spherical harmonics $Y_{lm}(\theta, \phi)$,[1] with coefficients $N_{lm}d_{lm}$, where constants N_{lm} are defined as the maximum values of $Y_{lm}(\theta, \phi)$:

$$N(\theta, \phi) = \sum_{l=0}^{\infty}\sum_{m=-l}^{l} N_{lm}d_{lm}Y_{lm}(\theta, \phi) \quad (13)$$

$$d_{lm} = N_{lm}^{-1}\int_0^{2\pi}\int_0^{\pi} N(\theta, \phi)\,Y_{lm}(\theta, \phi)\sin\theta d\theta d\phi. \quad (14)$$

[1]The $m = 0$ spherical harmonics explicitly used in this paper are: $Y_{00} = 1/\sqrt{4\pi}$; $Y_{20} = \sqrt{5/4\pi}(3\cos^2\theta - 1)/2$; $Y_{40} = \sqrt{9/4\pi}(35\cos^4\theta - 30\cos^2\theta + 3)/8$.

According to the extended mean value theorem for a definite integral (Fadell and Fadell, 1970), the values of d_{lm} are always between 1 and the ratio of the minimum and maximum values of $Y_{lm}(\theta, \phi)$.

In the ideal case, the dichroic factor $\gamma = 0$. In this case, the θ and ϕ dependence of the terms in Eq. 8 are written as a sum of Y_{00} and Y_{2m}, $m = -2, 2$, and substituted in Eq. 7 and then in Eq. 12. Eq. 13 is then inserted into Eq. 12, with $f = 1$. The integration is performed using the orthogonality properties of the Y_{lm}'s. Using $d_{00}N_{00} = 1/\sqrt{4\pi}$, which follows from Eqs. 11 and 13, and defining a normalized fluorescence $\mathcal{F}(\psi) = F(\psi)/F(\psi_0)$, where ψ_0 is the angle at which $F(\psi)$ is a maximum, it is found that

$$\mathcal{F}(\psi) = 1 + B(\cos^2\psi - \cos^2\psi_0) + C(\sin\psi\cos\psi - \sin\psi_0\cos\psi_0), \quad (15)$$

where

$$B, C = (b', c')/(a' + b'\cos^2\psi_0 + c'\cos\psi_0\sin\psi_0) \quad (16)$$

and

$$\begin{aligned} a' &= I_y[(1 - d_{20}) - 3(d_{22} - d_{2-2})/4]; \\ b' &= (I_x - I_y + I_z) + d_{20}(2I_z - I_x + I_y) \\ &\quad + 3(d_{22} + d_{2-2})(I_x - I_y)/4; \\ c' &= 3i[I_{yx}(d_{21} + d_{2-1}) + I_{xy}(d_{2-2} - d_{22})/2]. \end{aligned} \quad (17)$$

Parameters B, C, and ψ_0, obtained experimentally, are directly related to the coefficients d_{2m}, $m = -2, 2$, through Eqs. 16 and 17. The other expansion coefficients, d_{lm}, $l = 1, 3, 4, \ldots$, do not affect $\mathcal{F}(\psi)$. Thus, any two distributions $N(\theta)$ having the same values for the d_{2m}'s, but different values for d_{lm}'s when $l \neq 2$, will have the same experimental curve $\mathcal{F}(\psi)$ and the same measured values of B and C.

In analyzing the experimental results in this paper, we consider only azimuthally symmetric distributions $N(\theta)$. This is suggested by the measured value of C (zero) in that all azimuthally symmetric distributions would have zero C values (since d_{lm} for $m \neq 0$ are zero). It is further justified by the measured absence of dichroism in the fluorescence measured with epi-illumination (see Materials and Methods and Results). For an azimuthally symmetric distribution,

$$B = \frac{[(I_z - I_y + I_x) + d_{20}(2I_z + I_y - I_x)]}{[I_y(1 - d_{20}) + \cos^2\psi_0\{(I_z - I_y + I_x) + d_{20}(2I_z + I_y - I_x)\}]}, \quad (18)$$

where ψ_0 is 0° or 90° if the numerator is positive or negative, respectively. The parameter B depends only on the Y_{20} moment of the absorption dipole distribution, d_{20}. The coefficient d_{20} is sometimes referred to as the (sole) "order parameter."

In the nonideal case when γ deviates from zero appreciably, a more complicated treatment that accounts for an $f(\theta)$ of the form shown in Eq. 10 can be developed. The θ, ϕ dependence of the product $\mathcal{A}(\theta, \phi)f(\theta)$ is written as a sum of terms proportional to Y_{00}, Y_{2m}, $m = -2, 2$, or Y_{4m}, $m = -4, 4$; these terms are put into Eq. 12 along with Eq. 13. Again, the integral in Eq. 12 is done using the orthogonality properties of the Y_{lm}'s, and a normalized fluorescence $\mathcal{F}(\psi)$ is defined. $\mathcal{F}(\psi)$ is found to be of the form of Eq. 15. For an azimuthally symmetric distribution, $C = 0$, and

$$B = b'(\gamma)/[a'(\gamma) + b'(\gamma)\cos^2\psi_0], \quad (19)$$

where

$$\begin{aligned} a'(\gamma) &= I_y[1/3 - \gamma/15) - d_{20}(1/3 + \gamma/21) + d_{40}4\gamma/35]; \\ b'(\gamma) &= [(I_x - I_y)(1/3 - \gamma/15) + I_z(1/3 - \gamma/5)] \\ &\quad + d_{20}[(I_y - I_x)(1/3 + \gamma/21) + I_z(2/3 - 4\gamma/7)] \\ &\quad - d_{40}(2I_z + I_y - I_x)\,4\gamma/35. \end{aligned} \quad (20)$$

The parameter B depends both on the Y_{20} moment (d_{20}) and on the Y_{40} moment (d_{40}) of the absorption dipole distribution.

When the probes are randomly distributed, $N(\theta, \phi) = 1$ and $d_{20} = d_{40} = 0$. Using Eqs. 19 and 20 for $n = 1.334/1.5$, $\alpha = 70°$, and $\mathcal{E}_z = \mathcal{E}_{z1}$, we find that $B = 0.19$ for $\gamma = 0$ and $B = 0.13$ for $\gamma = 0.10$ for randomly oriented samples.

Step Function Model

A model for the form of the dipole distribution $N(\theta, \phi)$ will in general contain one or more free parameters, to be determined from B and C. A useful model is one in which the dipoles are contained equally within an angular deviation of $2\Delta\theta$ about a certain angle θ_0 from the normal to the interface:

$$N(\theta, \phi) = \begin{cases} [4\pi\sin\theta_0\sin\Delta\theta]^{-1} & \theta_0 - \Delta\theta \leq \theta \leq \theta_0 + \Delta\theta \\ 0 & \text{otherwise} \end{cases}. \quad (21)$$

Parameters d_{20} and d_{40} are calculated for different values of θ_0 and $\Delta\theta$ by integrating Eq. 14, using Eq. 21. Parameter B is then calculated as a function of θ_0 and $\Delta\theta$ by using the calculated values of d_{20} and d_{40} and an appropriate value of γ in Eqs. 19 and 20. The results are shown in Fig. 2 for $\alpha = 70°$, $n = 1.334/1.5$, $\mathcal{E}_z = \mathcal{E}_{z1}$, and $\gamma = 0$. As shown, a measured value of B is consistent with a range of values of θ_0 and $\Delta\theta$ that form a line on a two-dimensional plot in θ_0 and $\Delta\theta$. For $B > 0.19$, all pairs $\Delta\theta, \theta_0$ consistent with a given B have about the same θ_0, but $\Delta\theta$ can range from 0° to θ_0. Thus, the measurements in this range are more sensitive to changes in θ_0 than in $\Delta\theta$. Plots similar to Fig. 2 have been constructed for $\gamma = 0.10$, $\mathcal{E}_z = \mathcal{E}_{z1}$ and for $\gamma = 0.44$ and $\mathcal{E}_z = \mathcal{E}_{z2}$, using Eqs. 19 and 20 and the values of d_{20} and d_{40} calculated from Eqs. 21 and 14 (results not shown). These plots are used in data analysis.

MATERIALS AND METHODS

Optics and Electronics

The purpose of the optical system is to measure the fluorescence from a supported phospholipid monolayer when excited with a totally internally reflected laser beam of variable polarization. Similar optical systems have been described in detail (Burghardt and Axelrod, 1981; Weis et al., 1982; Thompson and Axelrod, 1983) and reviewed (Axelrod et al., 1984). As shown in Fig. 3 *a*, the 488-nm line of an argon ion laser (model 265; Spectra-Physics Inc., Mountain View, CA) at ~20 μW is passed through a polarization rotator (Spectra-Physics Inc.) and is then directed through a focusing lens and into a hemicylindrical quartz prism (Harrick Scientific, Ossining, NY). As shown in Fig. 3 *b*, the hemicylindrical prism rests on top of, and is in optical contact with, the back of a supported monolayer. The supported monolayer rests on top of a 50-μm Teflon spacer (Nicholson Precision, Gaithersburg, MD) in a plastic dish that has its bottom replaced by a coverslip of thickness 80–130 μm (Arthur H. Thomas Co., Philadelphia, PA), sealed in with encapsulating resin. The beam is incident on the slide/water interface at 70° from the vertical, so that it totally internally reflects at the interface. Fluorescence is collected from below the coverslip with a 63-magnification, 1.4-NA oil immersion objective (Carl Zeiss, Inc., New York). The fluoresence passes through a filter block to a photomultiplier (C31034A02; RCA Electro-Optics & Devices, Lancaster, PA). The output of the photomultiplier is counted for single durations of 0.1 s, at 10° increments of incident beam polarization.

In some experiments, the laser beam is passed through the polarization rotator and then into the epi-illumination portal of the microscope (see Fig. 3 *b*), and focused to a small spot on the sample. This optical arrangement is particularly sensitive to probe orientation with respect to the azimuthal angle ϕ. Fluorescence excited with epi-illumination is measured as a function of incident beam polarization as described above.

Profile of a Focused, Totally Internally Reflected Laser Beam

The evanescent electric field produced by the focused, totally internally reflected laser beam has been calculated as a function of x, y, and z, using previously described computer programs (Burghardt and Thompson, 1984*a*). In these calculations, $\alpha = 70°$, $n_1 = 1.334$, $n_2 = 1.5$, the lens exit pupil β is 5°, the lens focal length is 60 mm, and the beam radius is 0.625 mm. The evanescent intensity profile is of approximate elliptical Gaussian shape with $1/e^2$ widths in the x and y directions of 46.4 and 15.5 μm, respectively. The average (weighted according to local intensity) angular deviations D of the calculated evanescent electric field direction from that produced by a single, totally internally reflected plane wave are: $\psi = 0°$, $x = 0$, $D = 0.04°$; $\psi = 0°$, $y = 0$; $D = 0.6°$; $\psi = 90°$, $x = 0$, $D = 0.1°$; $\psi = 90°$, $y = 0$, $D = 0.0002°$. Eqs. 1–3 thus accurately describe the focused totally internally reflected laser beam.

Supported Phospholipid Monolayers

Monolayers consisted of L-α-dipalmitoyl phosphatidylcholine (DPPC; Sigma Chemical Co., St. Louis, MO) or L-α-dimyristoyl phosphatidylcholine (DMPC; Calbiochem-Behring Corp., La Jolla, CA) and 2 mol % of either (see Fig. 4) 1-acyl-2-(12-[*N*-(-7-nitrobenzo-2-oxa-1,3-diazol-4-yl)]-aminododecanoyl)-phosphatidylethanolamine (chain-labeled NBD-PE, Avanti Polar Lipids, Birmingham, AL) or *N*-(7-nitro-2-oxa-1,3-diazol-4-yl)-L-α-dipalmitoylphosphatidylethanolamine (head-labeled NBD-PE, Avanti Polar Lipids), or NBD-PE-peptide. NBD-PE-peptide was synthesized from chain-labeled NBD-PE and the peptide Pro-His-Pro-Phe-His-Phe-Phe-Val-Tyr-Lys (Peninsula Labs, Inc., San Carlos, CA) (Burton et al., 1975, 1980), as previously described (Thompson et al., 1984).

Glass microscope slides were cleaned and alkylated as previously described (Thompson et al., 1984), except that after sonication the slides were submerged in chromic acid for at least 30 min and then rinsed with

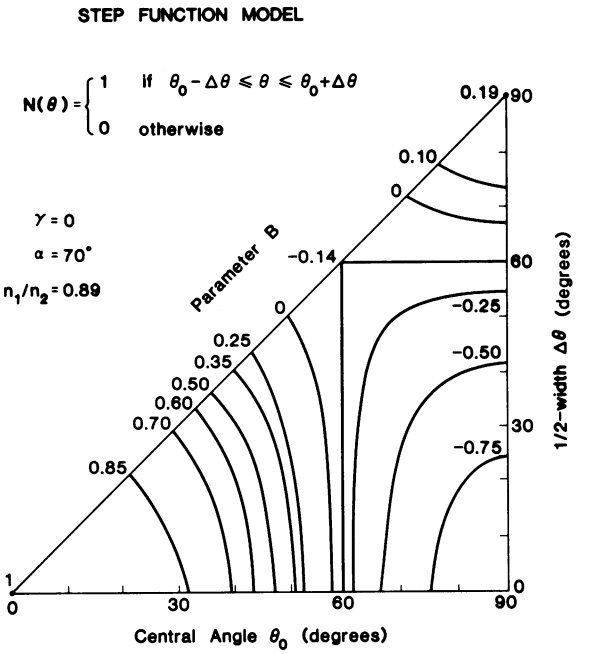

FIGURE 2 Values of the parameter B. The distribution of dipoles $N(\theta, \phi)$ is given by Eq. 21, with $\theta_0 = 0°$ to 90° and $\Delta\theta = 0°$ to θ_0. The incidence angle α is 70°; the relative refractive index $n = n_1/n_2$ is 1.334/1.5 = 0.889; the dichroic factor $\gamma = 0$; and the dipole is in the n_1 medium ($E_z = E_{z1}$). Many pairs of θ_0 and $\Delta\theta$ are consistent with a given value of B.

acetone/ethanol. Monolayers were prepared at the interface of air and aqueous solution and transferred to alkylated slides, as previously described (von Tscharner and McConnell, 1981*a*,*b*; Thompson et al., 1984). For peptide-lipid and chain-labeled NBD-PE in DMPC, the solution was 0.01 M $NaPO_4$, 0.14 M NaCl, pH 7.4 (phosphate-buffered saline [PBS]) and the spreading solvent was chloroform/methanol/water (65:25:4). For DPPC monolayers, the solution was water and the spreading solvent was hexane/ethanol (9:1). Slide-supported monolayers were transferred to the sample holder under water before transferring to the microscope stage. Fluorescence was measured no longer than 30 min after transfer. All experiments were done at room temperature. Control samples of randomly oriented fluorophores consisted of 1 μg/ml fluorescein isothiocyanate (Sigma Chemical Co.) in ethyl alcohol and nonalkylated glass slides.

Angle between the Absorption and Emission Dipole of NBD

Solutions of 5×10^{-8} M chain-labeled NBD-PE in encapsulating resin were cured in disposable polystyrene fluorescence cuvettes. Fluorescence intensities parallel and perpendicular ($F_\parallel$, $F_\perp$) to the excitation polarization were measured to determine the angle between the absorption and emission dipoles, ν, as given by (Cantor and Schimmel, 1980):

$$[F_\parallel - F_\perp]/[F_\parallel + 2F_\perp] = (3\cos^2\nu - 1)/5. \qquad (22)$$

Angle ν was found to equal 25°. This value is a maximum value because any residual probe motion or misalignment in the optics would depolarize the measured fluorescence. A nonzero ν affects only the model-dependent data analysis and only for large γ.

Data Analysis and Curve Fitting

Dichroism in the collection optics was corrected for by finding multiplicative factors for the baseline, at each ψ, that would give an $F(\psi)$ of the form

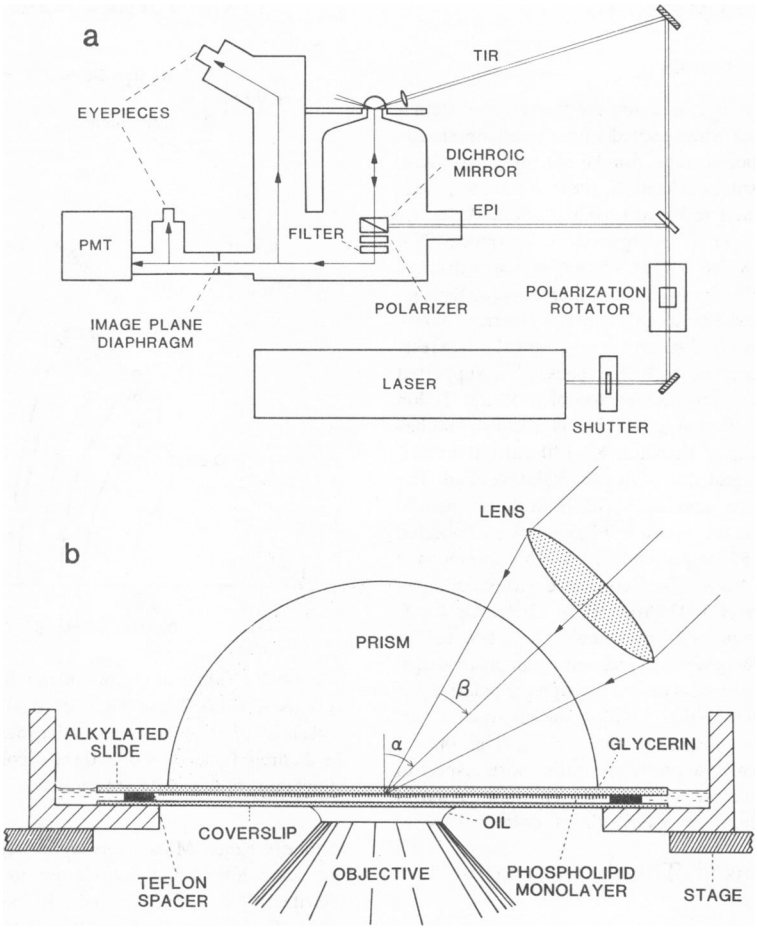

FIGURE 3 Optical apparatus. (*a*) The laser beam passes through a shutter and a polarization rotator and is then incident on the sample mounted on an inverted microscope. The sample is illuminated either by total internal reflection or epi-illumination. Light collected by the objective passes through either a colored glass filter or a dichroic mirror, and then (in some experiments) through a polarizing film. The filtered light is directed either to an eyepiece, through an image plane diaphragm and to a secondary eyepiece, or through the diaphragm to a photomultiplier. (*b*) The bottom of a plastic dish is replaced by a coverslip. The dish supports a teflon spacer and then an alkylated slide covered with a phospholipid monolayer. The slide is optically coupled to a quartz prism with glycerin, and the assembly is mounted on an inverted microscope equipped with a high-aperture oil immersion objective. A laser beam passes through a focusing lens with exit pupil β and is incident on the slide/water interface at angle α, where it totally internally reflects.

of Eq. 15 with $C = 0$ and $B = 0.13$. The monolayer curves were then multiplied by these factors and divided by the maximum value $F(\psi_0)$. The value of ψ_0, determined by inspection, was always equal to 0° for monolayer curves. Values for the parameters B and C were obtained from each normalized curve $\mathcal{F}(\psi)$ by a curve-fitting procedure (Burghardt et al., 1983).

$F(\psi)$, obtained for fluorescence excited with epi-illumination, was analyzed by inspection. Considerable dichroism was introduced in the collection optics by the presence of the dichroic mirror necessary for epi-illumination measurements.

RESULTS

Fig. 5 *a* shows two typical curves $F(\psi)$ for fluorescent-labeled phospholipids in supported monolayers excited with the evanescent field.

Fig. 5 *b* shows the average value of B for chain-labeled and head-labeled NBD-PE in DPPC monolayers under deionized water for coating pressures of 10–40 dyne/cm. B for the chain-labeled probe is approximately constant with an overall average of 0.68 ± 0.01; B for the head-labeled probe drops from 0.60 ± 0.01 at 10 dyne/cm to 0.25 ± 0.01 at 40 dyne/cm. Each measured value of C was nearly zero.

The value of B for chain-labeled NBD-PE and NBD-PE-peptide in DMPC monolayers under PBS does not vary for coating pressures of 20–40 dyne/cm. The overall average values of B are: NBD-PE, 0.70 ± 0.01; NBD-PE-peptide, 0.68 ± 0.01. Each measured value of C was nearly zero.

For samples excited with epi-illumination, no difference was observed between monolayers and randomly distributed fluorophores.

DISCUSSION

In three recent works (Lösche et al., 1983; Peters and Beck, 1984; McConnell et al., 1984), coexisting solid and fluid domains have been observed by fluorescence microscopy in DPPC monolayers at the air/water interface.

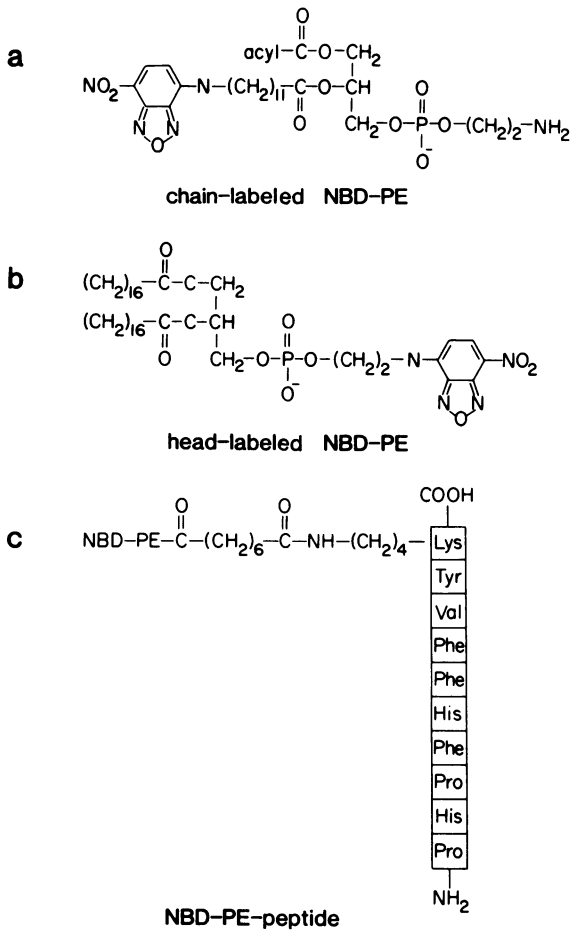

FIGURE 4 Fluorescent lipids. (*a*) Chain-labeled NBD-PE (from egg); (*b*) head-labeled NBD-PE (dipalmitoyl); (*c*) NBD-PE-peptide.

Chain-labeled NBD-PE partitions mainly into the fluid domains, whereas head-labeled NBD-PE (dipalmitoyl) partitions into both types of domains (McConnell et al., 1984). With increasing surface pressure from 5 to 40 dyne/cm, the solid domains increase in area and the fluid domains decrease in area.

Consistent with the partitioning behavior of the probes, the measurements of B for NBD-PE in DPPC monolayers suggest that the orientation distribution of chain-labeled NBD-PE does not change, whereas the orientation distribution of head-labeled NBD-PE does change with the surface pressure at coating. Based on plots similar to Fig. 2, with the appropriate field $\mathcal{E}_{z1}$ or $\mathcal{E}_{z2}$ and the appropriate value of γ, we find that the measured value of B for the chain-labeled probe is consistent with a distribution of the form of Eq. 21 with $\theta_0 = 34.0°$, $\Delta\theta = 0°$ to $\theta_0 = \Delta\theta = 24.5°$. Similarly, the measured value of B for head-labeled NBD-PE at 10 dyne/cm is consistent with $\theta_0 = 44.0°$, $\Delta\theta = 0°$ to $\theta_0 = \Delta\theta = 33.0°$, and at 40 dyne/cm it is consistent with $\theta_0 = 53.5°$, $\Delta\theta = 0°$ to $\theta_0 = \Delta\theta = 43.0°$. By examining plots similar to Fig. 2, it can be seen that B is more determined by θ_0 than by $\Delta\theta$. For values of B between 0.25 and 0.75, all pairs of $\Delta\theta$, θ_0 consistent with a given value of B have similar values of θ_0, but values of $\Delta\theta$ ranging from 0° to θ_0. Also, the value of θ_0 refers to the orientation of the NBD absorption dipole, which is not known with respect to the NBD molecule. Therefore, the main conclusion is that the average dipole polar angle and/or the average deviation from this angle increases from chain-labeled to head-labeled at low pressure to head-labeled at high pressure.

The measured value of B for chain-labeled NBD-PE, which partitions into the fluid domains, does not change with pressure. This suggests that $N(\theta)$ does not change, and thus that the local environment of the probe does not change. This would occur if the fluid domains had low

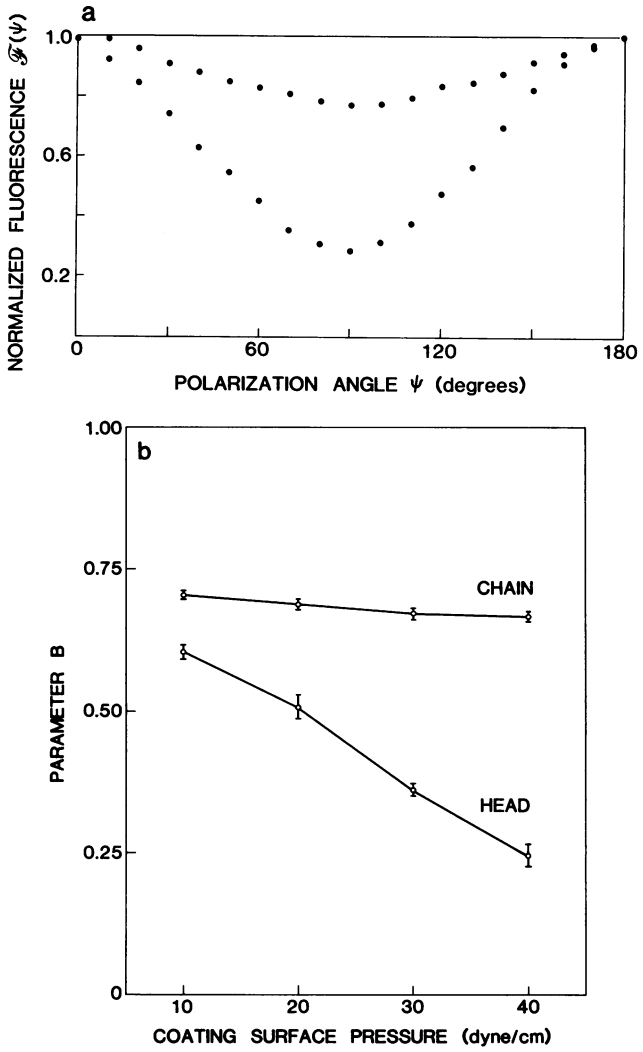

FIGURE 5 Absorption dichroism detected by fluorescence. (*a*) A typical single measurement of $\mathcal{F}(\psi)$, the fluorescence as a function of incident laser polarization ψ. The bottom curve was chain-labeled NBD-PE in DPPC ($B = 0.70$) at 10 dyne/cm and the top curve was head-labeled NBD-PE in DPPC at 40 dyne/cm ($B = 0.25$). (*b*) Average measured values B for (top curve) chain-labeled NBD-PE and (bottom curve) head-labeled NBD-PE in DPPC monolayers as a function of the surface pressure at coating. Each point represents the average of at least five $\mathcal{F}(\psi)$ curves measured from each of at least three independently prepared monolayers.

compressibility. The high compressibility of the monolayer as a whole (von Tscharner and McConnell, 1981*a*) would in this case be accounted for by the formation of solid-phase domains.

The orientation distribution of head-labeled NBD-PE in DPPC is different in the solid and fluid domains. The decrease in B with increasing pressure implies that the average angle θ_0 is higher in the solid than in the fluid domains. The increase in angle may also be accompanied by a change in the range of orientations $\Delta\theta$ in the solid phase.

In an earlier work (Thompson et al., 1984), it was found that NBD-PE-peptide diffuses with a coefficient 10 times smaller than that of unconjugated lipid in DMPC monolayers at 24–28°C. This may arise from extensive peptide-monolayer interaction or from self-oligomerization of the peptide-lipid conjugates. The measured values of B for peptide-lipid and unconjugated lipid do not indicate that the NBD moieties on these two molecules have different orientations, and thus supply evidence against extensive peptide-monolayer interaction. It is also interesting that chain-labeled NBD-PE in fluid DMPC monolayers has a value of B similar to its value in fluid (low pressure) DPPC.

No measurable azimuthal asymmetry over the dimensions of the illuminated region (~1 μm) was measured for probes in monolayers excited with epi-illumination. Single crystal domains as large as 1 mm in DPPC monolayers on alkylated silicon have been observed with x-ray diffraction (Seul et al., 1983).

We have demonstrated that the fluorescence arising from fluorescent-labeled phospholipids in supported phospholipid monolayers, which are illuminated with a totally internally reflected laser beam, depends strongly on the polarization of the evanescent illumination. This "dichroic fluorescence" provides information about the orientation of the fluorescent molecules. Because evanescent illumination propagates along the interface, rotating the polarization provides information about the value of the polar angle of the absorption dipoles, with respect to the normal to the monolayer, which cannot be obtained by rotating the polarization of a beam propagating perpendicular to the monolayer.

Absorption dichroism as detected by fluorescence, using evanescent illumination, should prove useful in examining the orientation not only of fluorescent lipid probes in phospholipid monolayers, but also of fluorescent-labeled proteins specifically bound to or incorporated into planar membranes, and of biological molecules at the contact region between planar membranes and specifically bound immunological cells. It may also prove useful to extend these experiments to measure time-resolved orientation distributions of polar angles, either by using time-resolved fluorescence anisotropy or fluorescence recovery after photobleaching, in combination with polarized evanescent illumination. Finally, because the evanescent wave selectively illuminates only molecules that are within ~1,000 Å of the dielectric interface, polarized evanescent illumination can be used to selectively measure the order and dynamics of fluorescent-labeled molecules that are on the surface but in the presence of other fluorescent molecules in solution or in the system but not near the interface.

We thank Lynne Alexander for help in preparing the manuscript.

This work was supported by National Science Foundation grants PCM-8021993 and PCM-8313770 (to H. M. McConnell). N. L. Thompson is a Damon Runyon-Walter Winchell Cancer Fund Postdoctoral Fellow (593) and T. P. Burghardt is an American Heart Association Postdoctoral Fellow (82 071).

Received for publication 3 February 1984 and in final form 19 July 1984.

REFERENCES

Axelrod, D., T. P. Burghardt, and N. L. Thompson. 1984. Total internal reflection fluorescence. *Annu. Rev. Biophys. Bioeng.* 13:247–268.

Balakrishnan, K., F. J. Hsu, A. D. Cooper, and H. M. McConnell. 1982. Lipid hapten containing targets can trigger specific immunoglobulin E-dependent degranulation of rat basophil leukemia cells. *J. Biol. Chem.* 257:6427–6433.

Barlow, W. A. 1980. Langmuir-Blodgett films. *Thin Films Sci. Technol.* 1:1–288.

Borejdo, J., D. Assulin, T. Ando, and S. Putnam. 1982. Cross-bridge orientation in skeletal muscle measured by linear dichroism of an extrinsic chromophore. *J. Mol. Biol.* 158:391–414.

Born, M., and E. Wolf. 1980. Principles of Optics. Academic Press, Inc., New York. 36–51.

Brian, A. A., and H. M. McConnell. 1984. Allogeneic stimulation of cytotoxic T cells by supported planar membranes. *Proc. Natl. Acad. Sci. USA.* 81:6159–6163.

Burghardt, T. P. 1984. Model independent fluorescence polarization for measuring order in a biological system. *Biopolymers.* In press.

Burghardt, T. P., T. Ando, and J. Borejdo. 1983. Evidence for cross-bridge order in contraction of glycerinated skeletal muscle. *Proc. Natl. Acad. Sci. USA.* 80:7515–7519.

Burghardt, T. P., and D. Axelrod. 1981. Total internal reflection/fluorescence photobleaching recovery study of serum albumin absorption dynamics. *Biophys. J.* 33:455–467.

Burghardt, T. P., and N. L. Thompson. 1984*a*. Evanescent intensity of a focused Gaussian light beam undergoing total internal reflection in a prism. *Opt. Eng.* 23:62–67.

Burghardt, T. P., and N. L. Thompson. 1984*b*. Effect of planar dielectic interfaces on fluorescence emission and detection. Evanescent excitation and high-aperture collection. *Biophys. J.* 46:729–737.

Burghardt, T. P., M. Tidswell, and J. Borejdo. 1984. Cross-bridge order and orientation in resting single glycerinated muscle fibers studied by linear dichroism of bound rhodamine labels. *J. Muscle Res. Cell Motil.* In press.

Burton, J., R. J. Cody, J. A. Herd, and E. Haber. 1980. Specific inhibition of renin by an angiotension analog: studies in sodium depletion and renin-dependent hypertension. *Proc. Natl. Acad. Sci. USA.* 77:5476–5479.

Burton, J., K. Poulsen, and E. Haber. 1975. Competitive inhibitors of renin. Inhibitors effective at physiological pH. *Biochemistry.* 14:3892–3898.

Cantor, C. R., and P. R. Schimmel. 1980. Biophysical Chemistry Part II: Techniques for the Study of Biological Structure and Function. W. H. Freeman & Co., San Francisco, CA. 454–459.

Cartwright, G. S., L. M. Smith, E. W. Heinzelmann, M. J. Ruebush, J. W. Parce, and H. M. McConnell. 1982. H-2K^k and vesicular

stomatitus virus G proteins are not extensively associated in reconstituted membranes recognized by T cells. *Proc. Natl. Acad. Sci. USA.* 79:1506–1510.

Drexhage, K. H. 1974. Interaction of light with monomolecular dye layers. *Prog. Opt.* 12:163–232.

Fadell, E. R., and A. G. Fadell. 1970. Calculus. Van Nostrand Reinhold, New York. 182.

Fettiplace, R., L. G. M. Gordon, S. B. Hladky, J. Requena, H. P. Zingsheim, and D. A. Haydon. 1975. Techniques in the formation and examination of "black" lipid bilayer membranes. *Methods Membr. Biol.* 4:22.

Fluornoy, P. A., and W. J. Schaffers. 1966. Attenuated total reflection spectra from surfaces of anisotropic, absorbing films. *Spectrochim. Acta.* 22:5–13.

Hafeman, D. G., M. Seul, C. M. Cliffe, and H. M. McConnell. 1984. Superoxide release enhances photobleaching during immune attack on fluorescent lipid monolayer membranes. *Biochim. Biophys. Acta.* 722:20–28.

Hafeman, D. G., L. M. Smith, D. T. Fearon, and H. M. McConnell. 1982. Lipid monolayer-coated surfaces do not perturb the lateral motion and distribution of C3b receptors on neutrophils. *J. Cell Biol.* 94:224–227.

Hafeman, D. G., V. von Tscharner, and H. M. McConnell. 1981. Specific antibody-dependent interactions between macrophages and lipid haptens in planar lipid monolayers. *Proc. Natl. Acad. Sci. USA.* 78:4552–4556.

Harrick, N. J. 1967. Internal Reflection Spectroscopy. John Wiley & Sons, New York. 1–327.

Jackson, J. D. 1975. Classical Electrodynamics. John Wiley & Sons, New York. 391–397.

Kuhn, H., D. Mobius, and H. Bucher. 1972. Spectroscopy of monolayer assemblies. *In* Physical Methods of Chemistry, Part IIIB. A. Weissberger, and B. W. Rossiter, editors. John Wiley & Sons, Inc., New York. 577–702.

Lösche, M., E. Sackmann, and H. Mohwald. 1983. A fluorescence microscopic study concerning the phase diagram of phospholipids. *Ber. Bunsen-Ges. Phys. Chem.* 87:848–852.

McConnell, H. M., L. Tamm, and R. Weis. 1984. Periodic structures in lipid phase transitions. *Proc. Natl. Acad. Sci. USA.* 81:3249–3253.

Nakanishi, M., A. A. Brian, and H. M. McConnell. 1983. Binding of cytotoxic T-lymphocytes to supported lipid monolayers containing trypsinized H-2K^k. *Mol. Immunol.* 20:1227-1231.

Peters, R., and K. Beck. 1984. Translational diffusion in phospholipid monolayers measured by fluorescence microphotolysis. *Proc. Natl. Acad. Sci. USA.* 80:7183–7187.

Seul, M., P. Eisenberger, and H. M. McConnell. 1983. X-ray diffraction by phospholipid monolayers on single crystal silicon substrates. *Proc. Natl. Acad. Sci. USA.* 80:5795–5797.

Sinha, S. K., editor. 1980. Ordering in Two Dimensions. Elsevier/North-Holland, New York. 1–497.

Thompson, N. L., and D. Axelrod. 1983. Immunoglobulin surface-binding kinetics studies by total internal reflection with fluorescence correlation spectroscopy. *Biophys. J.* 43:103–114.

Thompson, N. L., A. A. Brian, and H. M. McConnell. 1984. Covalent linkage of a synthetic peptide to a fluorescent phospholipid and its incorporation into supported phospholipid monolayers. *Biochim. Biophys. Acta.* 722:10–19.

Uzgiris, E. E., and R. D. Kornberg, 1983. Two-dimensional crystallization technique for imaging macromolecules, with applications to antigen-antibody-complement complexes. *Nature (Lond.).* 301:125–129.

von Tscharner, V., and H. M. McConnell. 1981*a*. An alternative view of phospholipid phase behavior at the air/water interface. Microscope and film balance studies. *Biophys. J.* 36:409–419.

von Tscharner, V., and H. M. McConnell. 1981*b*. Physical properties of lipid monolayers on alkylated planar glass surfaces. *Biophys. J.* 36:420–427.

Watts, T. H., A. A. Brian, J. W. Kappler, P. Marrack, and H. M. McConnell. 1984. Antigen presentation by affinity purified I-A^d reconstituted in supported planar membranes. *Proc. Natl. Acad. Sci. USA.* In press.

Weis, R. M., K. Balakrishnan, B. A. Smith, and H. M. McConnell. 1982. Stimulation of fluorescence in a small contact region between rat basophil leukemia cells and planar lipid membrane targets by coherent evanescent illumination. *J. Biol. Chem.* 257:6440–6445.